Available online at www.sciencedirect.com
SCIENCE DIRECT®
Journal of Contaminant Hydrology 75 (2004) 1–29
JOURNAL OF Contaminant Hydrology
www.elsevier.com/locate/jconhyd

Displacement and sweep efficiencies in a DNAPL recovery test using micellar and polymer solutions injected in a five-spot pattern

Richard Martel[a,*], Alain Hébert[b], René Lefebvre[a], Pierre Gélinas[b], Uta Gabriel[a]

[a] *INRS-Eau, Terre et Environnement, Institut national de la recherche scientifique, Université du Québec, 880 Chemin Sainte-Foy, C.P. 7500, Sainte-Foy, Québec, Canada G1V 4C7*
[b] *Département de Géologie et de Génie Géologique, Université Laval, Québec, Québec, Canada G1K 7P4*

Received 31 December 2002; received in revised form 3 March 2004; accepted 25 March 2004

Abstract

Soil washing with micellar solutions is a promising alternative for the remediation of DNAPL source zones. As with any flushing technology, the success of soil washing with micellar solutions depends in a very large part on the ability of the solution to contact the contaminant (sweep efficiency) and then on the efficiency of contaminant removal once this contact is made (displacement efficiency). We report here on a field test where a micellar solution was used to recover a DNAPL in an open five-spot pattern in which polymer solutions were also injected before and after the washing solution to improve sweep efficiency. The washing solution formulation was optimised in the laboratory prior to the test to obtain good dissolution capacity. For a high-concentration and low-volume soil flushing remediation test such as the one performed (0.8 pore volumes of actual washing solution injected), slug sizing of the washing solution is critical. It was evaluated by an analytical solution. In a five-spot pattern, the displacement efficiency of the washing solution was observed to vary in the porous medium as a function of the radial distance from the injection well because: (1) the volume of the washing solution flowing through a section of the test cell changes (maximum close to the injection well and minimal at the pumping wells); (2) the in situ velocity changes (maximum at the wells and minimum between the wells) and; (3) the contact time of the washing solution with the NAPL changes as a function of the distance from the injection well. The relative importance of the recovery mechanisms, mobilisation and dissolution, was also observed to vary in the test cell. The reduced velocity increased the contact time of the washing solution with the DNAPL enhancing its dissolution, but the decrease of the capillary number caused less mobilisation. The washing process is much more extensive around the injection well. The use of

* Corresponding author.Tel.: +1-418-654-2683; fax: +1-418-654-2615.
E-mail address: Richard_Martel@inrs-ete.uquebec.ca (R. Martel).

0169-7722/$ - see front matter
doi:10.1016/j.jconhyd.2004.03.007

an injection-pumping pattern allowing a complete sweep of the remediated area is essential. Following a comprehensive characterisation, modeling is an efficient tool to design the injection-pumping scheme and to optimise injection and pumping rates providing the best areal sweep. The vertical sweep can be controlled by using a polymer solution (Xanthan gum). The polymer solution also has a positive effect on front stability between the solutions injected. The injection rate of the polymer solution that follows the washing solution must be kept minimal initially to prevent dilution of the washing solution by fingering.

Keywords: Sweep efficiency; Displacement efficiency; Washing solution; NAPL; Polymer; Xanthan; Five-spot pattern

1. Introduction

It is well-known from experience in the petroleum industry that polymer solutions can be injected during surfactant flooding to improve mobility control and to increase the overall sweep efficiency (Manning et al., 1983; Lake, 1989). Heterogeneities in reservoirs, often present as stratification of various permeability materials, can adversely affect the washing solution sweep efficiency, by creating preferential flow channels, thus leaving important nonswept zones in low-permeability layers. Along with heterogeneity, instability phenomena are the main problems leading to a low sweep efficiency. These instabilities lead to the formation of fingers of the displacing fluid into the displaced fluid. For aquifer remediation with in situ soil washing techniques, the same processes are observed. Viscous fingering occurs generally when the displacing fluid is less viscous than the displaced fluid, as is the case when water is used to displace a more viscous washing solution (Lake, 1989). Previous studies combining sand box experiments and polymer flooding were made to simulate fluid circulation in petroleum reservoirs (Wheat and Dawe, 1988; Wright et al., 1987; Wright and Dawe, 1983) or aquifers (Martel et al., 1998a; Robert et al., 2002). Sand box experiments showed that the injection of a xanthan solution behind a washing solution slug eliminates viscous fingering at the polymer/washing solution front due to a mobility ratio smaller than one. Xanthan solutions are non-Newtonian fluids. The shear thinning behaviour facilitates the injection because the liquid is much less viscous in the high flow velocity area around the injection well. Finally, a preflush step with a xanthan solution is advantageous before the injection of washing solution to limit its mobility in the most permeable unit and to prevent surfactant adsorption on solids.

In the last decade, numerous soil washing field tests were performed in aquifers for different NAPL types and under different hydrogeologic contexts (Simpkin et al., 1999). Dissolution was the preferred NAPL recovery mechanism for most of these tests (as for example, Blanford et al., 2001; Knox et al., 1997; Rao et al., 1997; Sahoo et al., 1998) whereas mobilisation or a combination of both mechanisms was used in some tests (e.g., Falta et al., 1999). Jawitz et al. (1998) reported LNAPL recovery as a microemulsion phase with no mobilisation. According to the literature, polymer solutions were used in only three other tests. The xanthan gum was added to the washing solution to increase its viscosity in the Fredricksburg (Virginia, USA) and the Hialeah County (Florida, USA)

tests (Simpkin et al., 1999). The xanthan gum was added also to obtain a more favourable mobility ratio between the washing solution and the NAPL, and to improve the sweep efficiency of the tested area. In the Laramie test (Wyoming, USA; Pitts et al., 1993), xanthan gum was added to the preflush, the alkali-flood, the surfactant solution and two driving solutions. All solution contained 1.05 g/l xanthan gum, except for the case of the second driving solution where xanthan gum concentration was lowered.

This paper is the second one documenting a field test performed at the Thouin Sand Pit (Martel et al., 1998d). The first paper presented the experimental set up and the recovery of NAPL in the test plot. This paper aims to document: (1) the areal and vertical sweep efficiency observed with the injected polymer and washing solutions in the five-spot delivery/pumping system used in the field and (2) the detailed NAPL recovery mechanisms observed in soil during this field test. This paper also presents a method to guide the optimal dimensioning of a small-volume and high-concentration washing solution slug injected in a radial delivery/pumping pattern.

2. Background

2.1. Sweep efficiency

The volumetric sweep efficiency (E_V) is related to the efficiency of an injection-pumping pattern and it is defined as the ratio of the volume of oil contacted by the washing solution or polymer solution to the volume of oil originally in place (Lake, 1989). E_V has a direct influence on recovery efficiency (E_R; Lake, 1989):

$$E_R = E_D E_V \tag{1}$$

where E_D is the displacement efficiency and is defined as the volume ratio of the displaced oil to the contacted oil. E_D is a function of the washing solution composition and the mechanisms of displacement (dissolution or mobilisation). The washing solution composition plays the leading role in the displacement efficiency (E_D), which combined with the E_V, controls the recovery efficiency (E_R). E_V can be decomposed in two factors: the areal sweep efficiency (E_A) and the vertical sweep efficiency (E_I) (Lake, 1989):

$$E_V = E_A E_I \tag{2}$$

where

$$E_A = \frac{\text{Area contacted by displacing agent}}{\text{Total area}} \tag{3}$$

and

$$E_I = \frac{\text{Cross} - \text{sectional area contacted by displacing agent}}{\text{Total cross} - \text{sectional area}} \tag{4}$$

E_A is a function of the injection-pumping pattern and the ratio of injection-pumping rate. E_A and E_I depend on fluid viscosity and on porous medium heterogeneity. E_I is influenced also by the fluid density. Fig. 1 is a schematic representation of the areal and

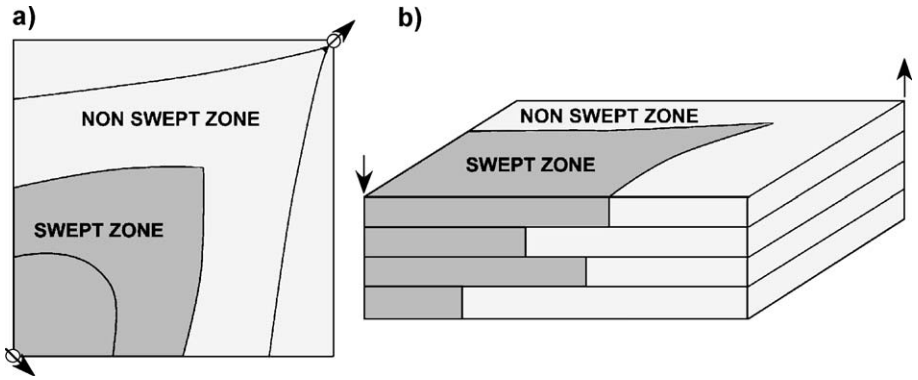

Fig. 1. Schematic representation of the two components of the volumetric sweep: (a) areal sweep; (b) vertical sweep (adapted from Lake, 1989).

vertical sweep from a liquid injected and pumped in a stratified geologic medium. The evaluation of E_A can be made by numerical simulation of the injection-pumping rate and by observation of samples collected in monitoring and pumping wells. Repeated experiments have shown that during water-flooding of petroleum reservoirs, E_V was around 40% to 60% for an E_R of about 30% (Lake, 1989). These experiments show the importance of using a polymer solution to enhance the volumetric sweep efficiency.

For a given pattern, vertical (E_I) and areal (E_A) sweep efficiencies are controlled by the mobility ratio (M) between the displacing fluid (λ_1) and the displaced fluid (λ_2).

$$M = \lambda_1/\lambda_2 \tag{5}$$

Fluid mobility (λ_i) is the ratio between the relative permeability of the porous medium (k_{ri}) and the fluid viscosity (μ_i).

$$\lambda_i = k_{ri}/\mu_i \tag{6}$$

When the relative permeability to the different injected fluids is the same, the mobility ratio is defined by the fluid viscosity ratio. For horizontal flow, a stable front is observed if the mobility ratio is smaller than 1 ($M<1$); that is, when the viscosity of the displacing fluid is greater than the viscosity of the displaced fluid. It follows from these considerations that the preflush polymer solution should have a viscosity greater than water viscosity but smaller than the washing solution viscosity, whereas in a push mode, the polymer solution should have a viscosity greater than the washing solution. Furthermore, density contrasts between the polymer and the washing solution should be minimal to avoid gravity effects which can induce over or under riding of the injected fluid relative to the displaced fluid (as observed by Grubb and Sitar, 1999, in horizontal sand column experiments). Xanthan gum is the selected polymer because of its shear thinning effect (Fig. 2). This means that the viscosity of the xanthan gum solution decreases with an increasing shear rate facilitating the flow in the high-velocity areas. Shear thinning is not

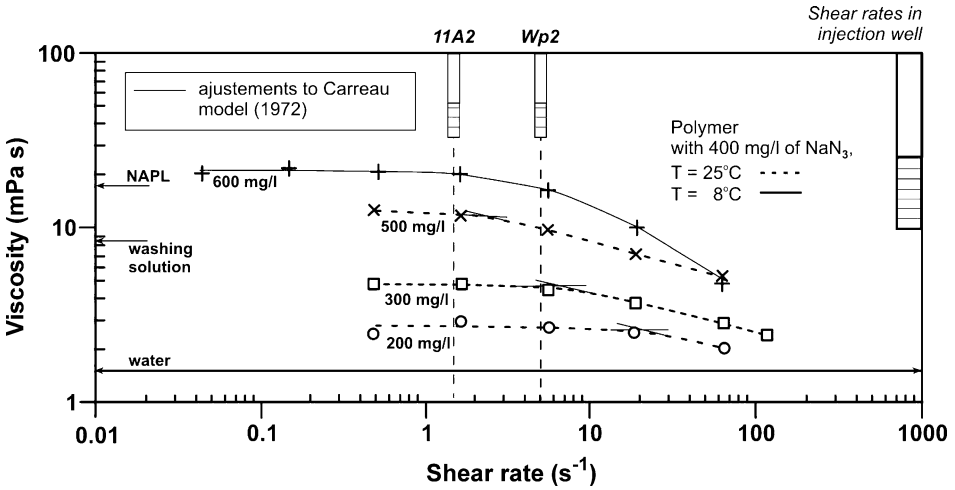

Fig. 2. Effect of shear rate on the viscosity of polymers. Adjustments to Carreau (1972) model are indicated.

observed with the CMC (sodium carboxymethylcellulose) solution that also needs a higher concentration to have the same viscosity as a xanthan gum solution.

Slug sizing of the washing solution is also very important in a high-concentration and low-volume approach such as the one used for the soil washing field test. For a radial injection configuration, there is a decrease in the slug thickness as a function of the distance from the injection well. The dilution of the injected slug by dispersion, both at its front and back, also affects the washing solution concentration. Because the washing solution is optimised for a specific composition, it is very important to preserve the integrity of the slug from the injection to the pumping wells. If the size of the slug is very small, its concentration will not remain at the initially injected concentration ($C/C_0 = 1$) everywhere in the cell. This may have a negative effect on the displacement efficiency and also on the recovery mechanisms involved. The effect of dilution of the injected solution concentration by dispersion can be assessed by a radial representation of the Ogata–Banks analytical solution (Ogata and Banks, 1961) representing miscible displacement and dispersion in a one-dimensional (1D) system.

2.2. Displacement efficiency

Mobilisation and dissolution are the two main DNAPL recovery mechanisms with in situ flushing using washing solutions. The mobilisation process for aquifer remediation should be used only when a continuous impermeable layer (clay, compact glacial till) is located under the contaminated zone (Pennell et al., 1996; Brandes and Farley, 1993) because of the danger associated to free-phase DNAPL downward migration as was observed by Ramsburg and Pennell (2001) in a two-dimensional sand box model after the introduction of a washing solution. To displace the DNAPL during flushing, viscous and buoyancy forces have to overcome the capillary forces, governed by interfacial

tensions (Mercer and Cohen, 1990). To quantify the forces acting in the mobilisation process, the trapping number N_T (Pennell et al., 1996) was defined as the sum of the capillary number N_C (viscous forces/capillary forces) and the Bond number N_B (gravity forces/capillary forces):

$$N_T = N_C + N_B = \frac{q\mu + k\Delta\rho\ g}{\sigma} \tag{7}$$

where q is the Darcy flux (m/s), μ is the dynamic aqueous phase viscosity (mPa·s), σ is the interfacial tension (IFT; mN/m), k is the intrinsic permeability (m^2), and $\Delta\rho$ is the density difference between the aqueous and NAPL phases (kg/m^3) and g (9.81 m/Δ^2) is the gravitational acceleration. With interfacial tensions reduced due to the presence of surfactants, alcohols or solvents in the washing solution, the trapped droplets of DNAPL become partially or entirely mobile. This results in an accumulation of a continuous organic phase ahead of the washing solution. Swelling of the organic phase by solvent and/or alcohol transfer contributes to a rise in organic phase saturation and relative permeability, favouring its displacement (Falta, 1998) and has the potential to decrease the density of the organic phase especially in the case of a DNAPL (Roeder et al., 2001). Lunn and Kueper (1999) did perform column experiments to show the in situ conditioning of the DNAPL before mobilising it. Sabatini et al. (2000) proposed a gradient approach increasing slowly the salinity in order to optimise the NAPL solubility while keeping the interfacial tensions between the contaminant and washing solution relatively high at the beginning of the experiment.

The ability of the washing solution to dissolve a DNAPL is primarily based on the nature of the solution components (alcohols, solvent or surfactants) and their concentration in the solution (active matter concentration). The more surfactant is added to the solution, the more micelles form and apparent DNAPL solubility increases (Shiau et al., 1994). Alcohols can also form aggregates that increase apparent DNAPL solubility in the washing solution (Quirion and Desnoyers, 1984). The density of the washing solution, initially and during DNAPL dissolution, is an important factor. A washing solution containing a high concentration of alcohol and/or solvent has an initial density lower than water and the potential for overriding the zone to be swept. Moreover, when dissolving a high-density DNAPL, the risk of downward migration of the washing solution is also of concern. As a consequence, the injected solutions densities must be controlled to avoid overriding or underriding of the injected solution relative to the displaced fluid. For example, the addition of a surfactant denser than water in these solutions may bring the density close to the water density. Furthermore, an injection/pumping strategy may be used to minimise density effects.

The construction of phase diagrams helps in predicting the dominant recovery mechanism associated to the composition and the concentration of a washing solution injected (Falta, 1998; St.-Pierre et al., 2004). At high active matter concentrations, however, both recovery processes usually coexist. Measuring the phase composition of the effluent during a field experiment is necessary to quantify the proportion of dissolved or/and mobilised DNAPL.

3. Methodology

3.1. Field test

The field experiment was made at the Thouin Sand Pit located 20 km north east of Montréal (Québec, Canada). This site was contaminated during the 1960s by several million litres of oil wastes dumped by trucks in ponds and sometimes burnt in the open. The site is characterized by an average 2 m layer of silty sand (the thickness varies from 1.6 to 2.4 m) underlain by a 30-m-thick layer of silty clay which acts as an impervious layer. At the experimental plot (approximately 4.17×4.17 m), the water saturated thickness of the silty sand layer varies from 0.9 to 1.4 m with an average thickness of 1.15 m. A discontinuous thin silt layer (10–15 cm in thickness) is located between 0.9 and 1.2 m depth close to the water table of this unconfined aquifer. The sand mineralogy is 82% quartz, 11% feldspar, 6% igneous rock fragments and 1% mica. The sand has an estimated porosity of 0.30, a particle size range of 0.05–2 mm with a medium particle diameter (d_{50}) of 0.4–0.8 mm, a specific surface area of 0.006 $m^2 \cdot g^{-1}$ and an organic matters content of $0.72 \pm 0.35\%$ (Table 1). The mean hydraulic conductivity from field slug tests in observation wells is 10^{-4} $m \cdot s^{-1}$. Groundwater flows east with a natural gradient of 0.009 and at a mean velocity of 95 $m \cdot year^{-1}$ (1.1 cm/h). The hydraulic conductivity decreases in the water saturated sand close to the upper silt layer and close to the bottom clay layer at the base of the formation. The DNAPL of the site is black and opaque, and has a characteristic odour. It is composed of a mixture of oil and solvents and has a density of 1020 $kg \cdot m^{-3}$ and a viscosity of 18 mPa·s. The average DNAPL initial concentration in the soil of the experimental plot was 55000 mg per kg

Table 1
Physical properties of the aquifer and the fluids and parameters of the field test

Aquifer properties		Fluids properties	
Hydraulic conductivity	10^{-4} m/s	Density (kg/m3)[a]	
Porosity	0.3	Water	998
Mean grain size	0.6 mm (sand)	DNAPL	1020
Organic matter content	0.7%	Washing solution	960
Specific surface	0.006 m^2/g	Polymer solutions	998
Saturated thickness	0.9 m to 1.4 m	Viscosity (mPa·s)	
Natural gradient	0.009	Water[a]	1.39
Groundwater velocity	95 m/y	DNAPL[a]	18
Test cell parameters		Washing solution[a]	8.5
Surface area	17.4 m^2	Polymer solution (200 mg/l)[b,c]	4
Spacing injection-pumping wells	3 m	Polymer solution (250 mg/l)[b,c]	5
Pore volume	6000 l	Polymer solution (500 mg/l)[b,c]	15
Injection rate	1 l/min	Polymer solution (600 mg/l)[a,b]	20
Pumping rate	2 l/min		
Initial DNAPL saturation	0.27		

[a] At 8 °C.
[b] Calculated viscosity at 8 °C by multiplying the measured viscosity at 25 °C by a factor of 1.4 (Martel et al., 1998a).
[c] At a shear rate of 1 s^{-1}.

of dry soils which represents a total of 1547 kg of DNAPL or a saturation of 0.27 (DNAPL volume/pore volume). The test cell had a five-spot injection-pumping pattern (Fig. 3). It is a 17.4 m^2 square delimited by four (4) recovery wells in the corners with a central injection well. The recovery wells were located at 3 m from the injection well. The washing experiment was performed in the water saturated sand unit. The water saturated pore volume (PV) of the cell was evaluated at 6000 l using the area of the cell (17.4 m^2) the average saturated thickness (1.15 m) and the porosity (0.30). The injection of the solutions was made by gravity and monitored by a flow meter at an average flow rate of 1 l/min. A packer was installed in the injection well just below the silt layer to prevent injection of fluids into the unsaturated zone. Peristaltic pumps were used to recover the effluents of the four extraction wells. The effluents were collected in an above ground reservoir. The cell was instrumented with eight (8) multilevel (three levels) observation wells and two (2) well points (2.5 cm in diameter and 30 cm long). The multilevel observation wells were built on site inside a 52 mm stainless steel screen installed in the saturated zone. Three nylon tubing (diameter of 6 mm), having the length needed for the sampling depth, were fixed to a stainless steel rod. The 10 cm bottom end of each tubing was pierced (2 mm holes) and covered with a piece of Nytex to prevent the sand pack from entering into the sampling tube. The rod containing the tubings was inserted into the screen and a sand pack of 15 cm length was placed around each

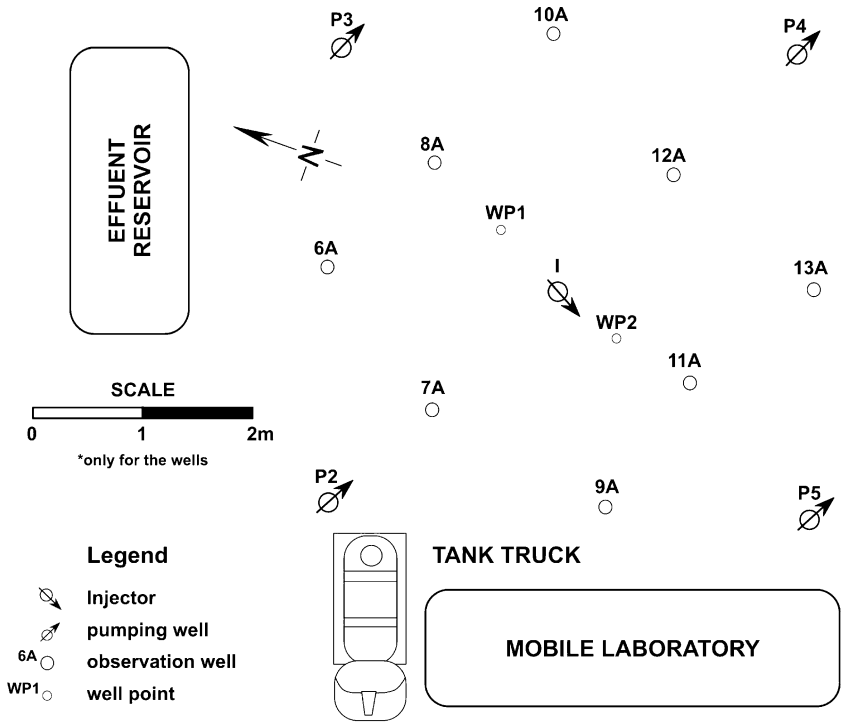

Fig. 3. Wells location and field set up.

sampling point. A 20-cm-long bentonite seal was also installed above each sand pack to prevent the circulation of the fluids between sampling points when sampling. The samples of fluid were taken from the observation wells with a 20 ml glass syringe that was decontaminated with dichloromethane, methanol and water before each sampling. Before sampling, the wells were purged by pumping one pore volume of the sand pack and the tubing.

The field test was performed during 3 weeks in November 1994. The used injection sequence is derived from enhanced petroleum recovery methods (Lake, 1989) but adapted to the special needs of the research on environmental remediation. The following fluids were injected in the given order (see Fig. 4): (1) water (0.3 PV) to reach the steady state for the flow system; (2) water (1.1 PV) containing a tracer (250 mg/l of chloride) for evaluation of front dispersion; (3) a preflush polymer solution (0.6 PV) made of 200 mg/l of xanthan in water to limit preferential flow of the washing solution in the more permeable layers and also to avoid preferential adsorption of washing solution ingredients onto sediments (Martel et al., 1998c)—a tracer (250 ppm of bromide) was added to this solution in order to observe the front stability; (4) washing solution (0.8 PV) containing a mixture of alcohol, surfactant and solvent in water to recover the trapped NAPL; (5) a postflush polymer solution (1.7 PV) of decreasing viscosity (0.74 PV at 600 mg/l, 0.48 PV at 504 mg/l and 0.46 PV at 250 mg/l of xanthan) with a tracer (250 mg/l of bromide) to push the washing solution out of the porous medium; (6) water (1.5 PV) to remove the polymer as much as possible because it is a preferential carbon source for bacteria and delays biodegradation of washing solution ingredients remaining in the porous medium (Roy et al., 1995); (7) water (1 PV) with acclimated autochthonous bacteria and nutriments.

The rinse cycle only consisted of several pore volumes of polymer solution and water. It should have included the injection of an alcohol–surfactant solution prior to the polymer solution to recover the solvent used in the washing solution as demonstrated in previous

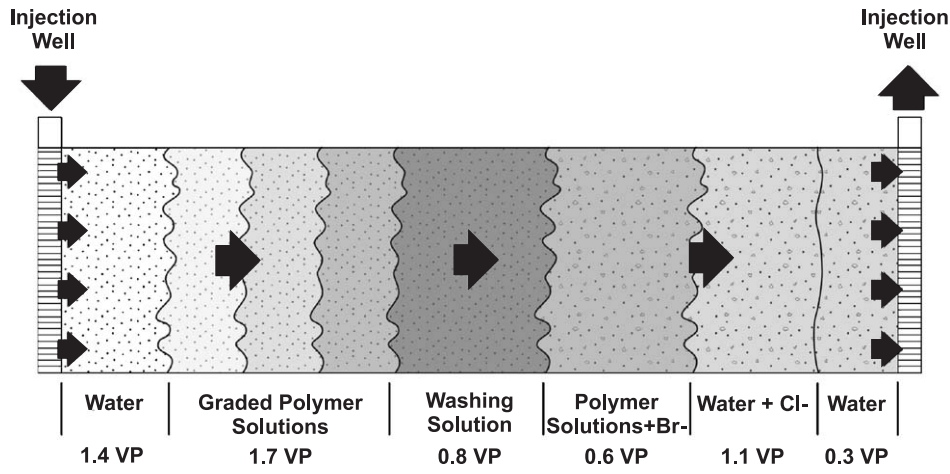

Fig. 4. Schematic representation of the injection sequence used in the field. Linear geometry and not to scale.

lab experiments (Martel et al., 1998c). Unfortunately, this step had to be omitted because of budget concerns and time limits.

The xanthan gum was selected as polymer for its nontoxicity and its shear thinning property which is favourable for the high velocities around the wells. Table 2 shows the mobility ratios of the injected fluids during the field test. The mobility ratio between the washing solution and the preceding polymer solution is 0.47 and between the postflush polymer solution and the washing solution it is 0.43. These ratios maintain a stable front between fluids. For the solution following the polymer of 600 mg/l, it is required to have a mobility ratio higher than one because of the rinsing steps. It is possible to limit the unfavourable effects by decreasing gradually the viscosity of the polymer solution.

The washing solution was composed of a surfactant (12% Hostapur SAS from Clariant), an alcohol (12% *n*-butanol) and two solvents (19% D-limonene; 5% toluene). All proportions are expressed in mass %. The density of this solution is 959.7 $kg \cdot m^{-3}$ and its viscosity is 8.5 mPa·s. Over 2000 fluid samples were taken from the 26 observation wells in the cell during the field test. Because it was very costly to analyse all collected samples, analyses were conducted on a cross-section between the injector and the pumping wells P5 and P3. This cross-section includes a well point (WP2) at 0.65 m from the injector and an observation well with three sampling levels (11A2) at 1.4 m from the injector (Fig. 3). The analysis of the surfactant was made with a titration method (Zhen Cao, 1978). A gas chromatograph (HP 6890) was used for alcohol and solvents determination. An ionic chromatograph (Dionex DX-100) was used for bromides and chlorides analysis and a spectrophotometer (HACH DR/200) at 500 nm for the DNAPL concentration determination in dichloromethane.

3.2. Analytical and Numerical modeling

The slug sizing of the washing solution is not only related to the volumetric sweep efficiency but also to the displacement efficiency. A five-spot pattern was used for the field test. With this pattern, the thickness of the "cylinder" representing the injected washing solution slug decreases as a function of the distance from the injector. Furthermore, dispersion at the edges of the washing solution slug can affect its integrity by shrinking the thickness over which concentration remains at the injected value. It is critical to evaluate the minimum size of the washing solution slug that must be injected to still have a slug

Table 2
Mobility ratio of the injected fluids relative to the previous injected fluid

Injected fluids (in injection order)	Viscosity (mPa·s)[a]	*M*
Water	1.39	1.00
Water with tracers	1.39	1.00
Preflush polymer solution (200 mg/l)	4.00	0.35
Washing solution	8.50	0.47
Postflush polymer solution (600 mg/l)	20.00	0.43
Postflush polymer solution (504 mg/l)	15.00	1.33
Postflush polymer solution (250 mg/l)	5.00	3.00

[a] Measured or calculated at 8 °C (see Table 1).

present in the soil at initially injected concentration once it reaches the pumping wells. The slug sizing of the washing solution was determined using the analytical solution of Ogata and Banks (1961), adapted to a radial geometry to predict the concentration profile in the soil for different theoretical volumes of slugs injected (see the Appendix for adaptation of the 1D Ogata–Banks solution to a radial geometry). In order to represent the slug the two fronts of increasing and decreasing concentration were superposed. An estimated porosity of 0.3, a hydraulic conductivity of 10^{-4} m/s evaluated from field slug tests and a dispersivity of 0.015 m were used for the calculation (Peclet Number of 200). The dispersivity is in agreement with Gelhar et al. (1985) who observed that a ratio of 100 exists between the scale of the test (3 m) and the longitudinal dispersivity.

The areal sweep efficiency of the five-spot pattern used for the field test was also predicted by numerical modeling. Different injection and pumping rates for the wells were simulated under steady state with MODFLOW (McDonald and Harbaugh, 1988). Modeling also provided information on the fluid velocity inside the porous medium of the tested cell. The numerical grid elements used were 0.25 by 0.25 m wide inside the test plot and enlarged progressively to the boundaries located 66 m upstream and downstream of the test plot and at 46 m on both of the other sides. The constant head boundaries upstream and downstream were used to simulate the natural groundwater gradient of 0.009, and no flow boundaries were fixed on the two other sides of the domain. Well locations, total aquifer thickness (1.2 to 2 m) for the modeled area (0.9 to 1.4 m in the experimental plot), hydraulic conductivity (10^{-4} m/s) and porosity (0.3) used in the model were derived from field data. Particle tracking was made with 400 or 100 particles injected. The pumping rate of the four pumping wells was fixed at 0.5 l/min by well. The same inputs were used for all the simulations. The only parameter varied in the simulations is the injection rate that changed from 0.5 to 1.0 and 2.0 l/min.

4. Results of modeling

4.1. Washing solution slug size determination

When soil washing is done using micellar solutions with a low solution volume at a high active matter concentration, such as in the described field test, it is critical to make sure that the volume of injected washing solution is large enough to reach the initially injected concentration over the entire porous medium treated. This is important because the developed washing solution is optimised to have the maximum efficiency at its injected concentration. In situ washing solution concentrations were predicted for different time steps using Ogata and Banks's (1961) solution modified for a radial geometry (Fig. 5a, b and c). On the y-axis, in situ washing solution concentrations are represented as a relative concentration C/C_0 where C_0 is the injected concentration. The x-axis represents the normalised radial distance (r/R) where r is the distance to the injection well and R the radius of the treated cell up to the pumping wells. Therefore, the origin corresponds to the position of the injection well and 1 to the position of a pumping well. A washing solution slug that occupies 25% of the pore volume (0.25 PV) of the test plot is not sufficient to

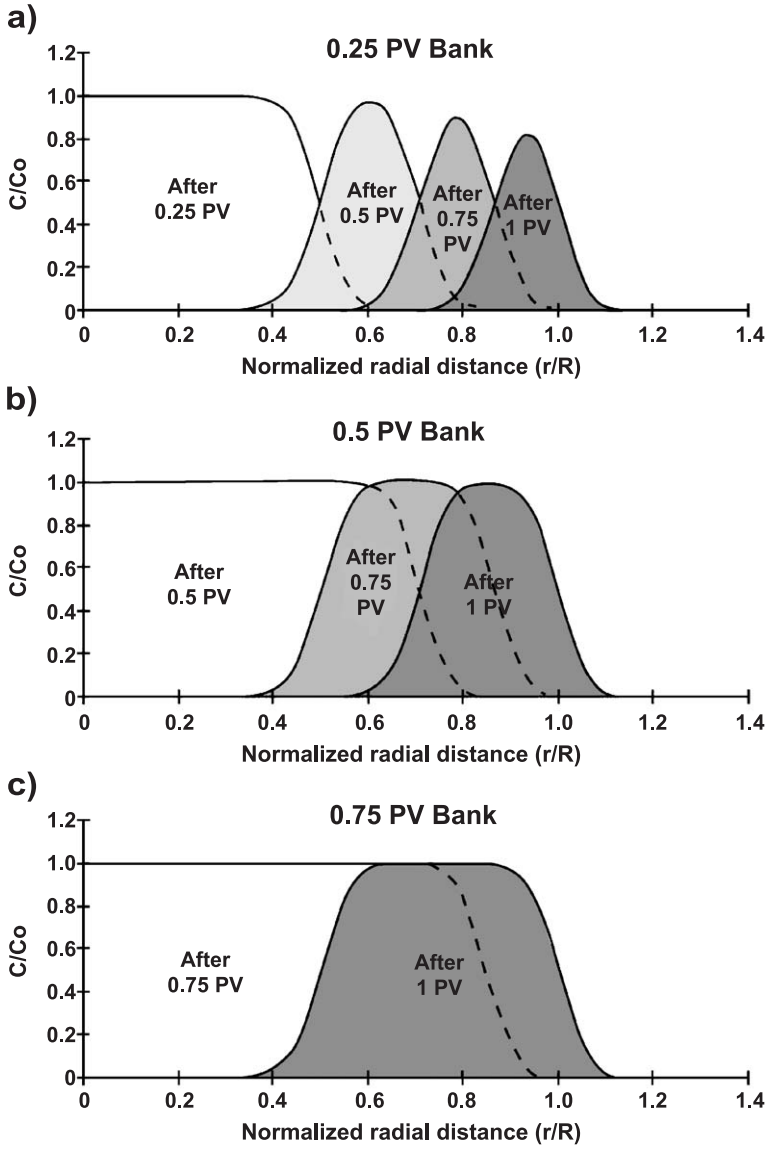

Fig. 5. Evolution of the (a) 0.25 PV slug, (b) 0.50 PV slug and (c) 0.75 PV slug.

flush the entire cell with the injected concentration (Fig. 5a). At the pumping well, the maximum active matter concentration (C) in the washing solution reached 80% of the injected concentration (C_0). When the injected washing solution volume is doubled to 50% of the pore volume, it is predicted that only 0.15 PV of the slug will remain at the initially injected concentration when the slug reaches the pumping well (Fig. 5b). This corresponds to only 8% of the normalised radial distance between the injector and the pumping well.

Finally, the injection of 75% of the pore volume washing solution provides 0.47 PV of an intact washing solution (with $C/C_0 = 1$) arriving at the pumping well (Fig. 5c). The thickness of the undiluted washing solution equals 27% of the normalised radius of the cell when solution breakthrough occurs at the pumping well. Based on this simulation, a volume of 0.8 PV of washing solution was injected during the field test. This is predicted to cause an intact washing solution slug of about 0.5 PV arriving at the pumping wells. A larger volume of washing solution was not used for the field test because its objective was not to fully recover all the DNAPL present within the test cell but rather to document the processes responsible for DNAPL recovery under a realistic field situation. The use of a relatively modest volume of washing solution also allowed a shorter field test to be carried out.

For a radial injection pattern, the volume of washing solution flowing through a cylindrical section of the test cell decreases nonlinearly as a function of the distance from the injection well [Eq. (8)].

$$\frac{V}{A} = \frac{V}{2\pi r b} \tag{8}$$

where V is the volume of washing solution injected, r is the radial distance from the injector, and b is the saturated thickness of the aquifer.

Fig. 6 shows that, for 5 m^3 (0.8 PV of the cell) of washing solution injected, the volume crossing a cylindrical surface area is 1.36 m^3/m^2 at a radial distance of 0.65 m (WP2) from the injector and 0.63 m^3/m^2 at a radial distance of 1.4 m (11A2).

This implies that the washing process is much more extensive around the injection well than near pumping wells. Thus, the washing efficiency of the washing solution can be expected to vary in the porous medium as a function of the radial distance from the injection well. The washing efficiency may be related to both, displacement and dissolution. A line drive pattern would have to be used to reduce the effect of this injection geometry and to obtain a more uniform flushing of the porous medium throughout the experimental plot. Fig. 7 shows the calculated velocity and the calculated shear rates profiles in the porous medium between the injection well and a pumping well for the used radial pattern. The velocity values were obtained from the numerical modeling of the hydraulic head of the five-spot pattern of the field test under steady state with

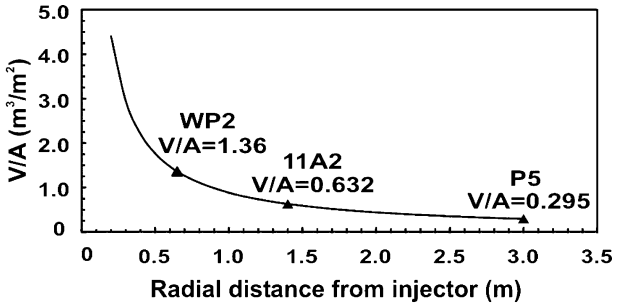

Fig. 6. Equivalent pore volume injected as a function of the distance from the injection well.

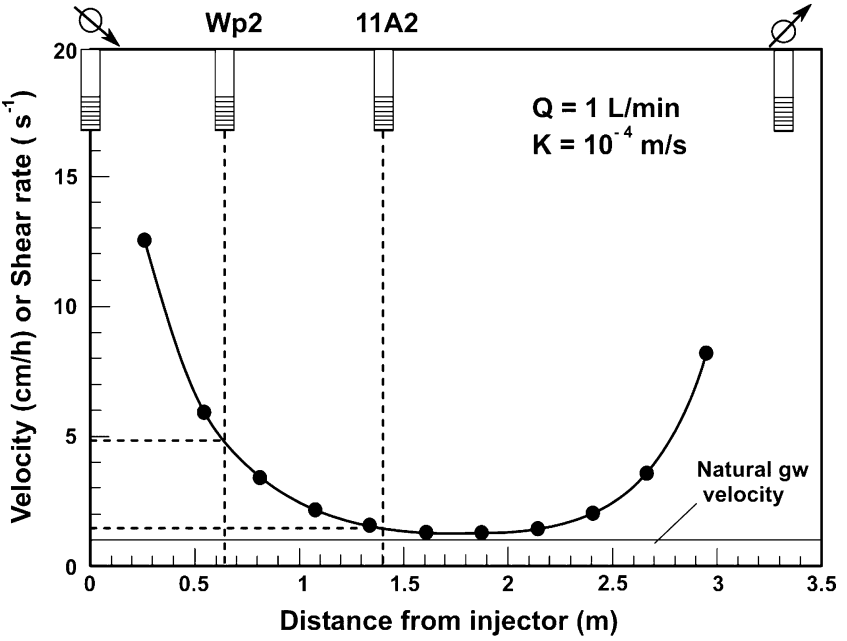

Fig. 7. Velocity of washing solution as a function of the distance from the injection well.

MODFLOW. The shear rates were calculated according to Eq. (9) from Chauveteau and Zaitoun (1981). In porous media, the shear rate (Υ) is a function of the fluid velocity (v_{fluid}), the porosity (n), the intrinsic permeability (k) and the parameter (φ) that can be fixed at 1.7 for a medium sand.

$$\Upsilon = \varphi(4\ v_{\text{fluid}})/(\sqrt{}(8k/n)) \tag{9}$$

The in situ fluid velocity and shear rate are maximum at the wells and minimum between the wells. This condition has an effect on the displacement efficiency because the contact time of the washing solution with the NAPL changes. This varied contact time can modify the proportions of the recovery mechanisms involved (see section below).

4.2. Areal sweep efficiency (E_A)

Fig. 8a to c show the particle tracking flow patterns simulated for the test cell for different injection rates. The pumping rate applied at each of the four wells is fixed at 0.5 l/min in all three cases. The parameter that varied between cases is the injection rate in the central injection well that goes from 0.5 to 1.0 and 2.0 l/min, respectively for Fig. 8a to c. The natural horizontal gradient of 0.009 induces a groundwater flow from P5 to P3. Fig. 8a shows the flow pattern when the injection rate is 0.5 l/min (injection/pumping

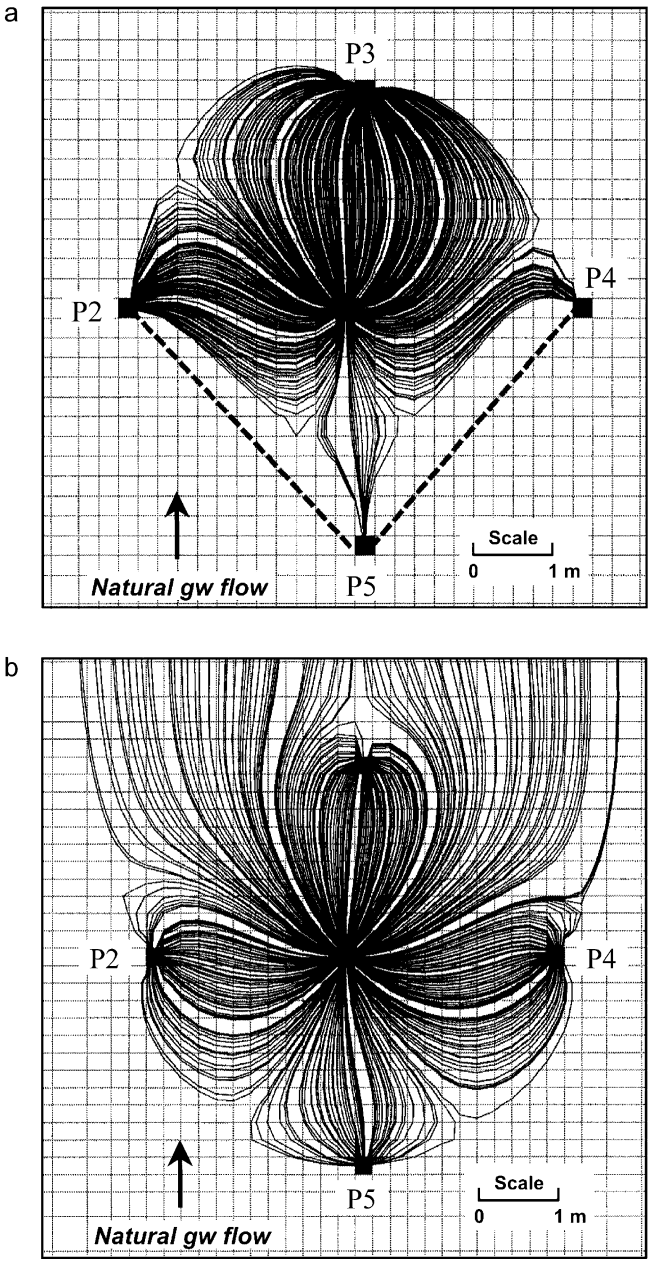

Fig. 8. (a) Particles tracking for an injection-pumping rate ratio of 1:4. (b) Particles tracking for an injection-pumping rate ratio of 1:1. (c) Particles tracking for an injection-pumping rate ratio of 1:2 (time steps of 20 h).

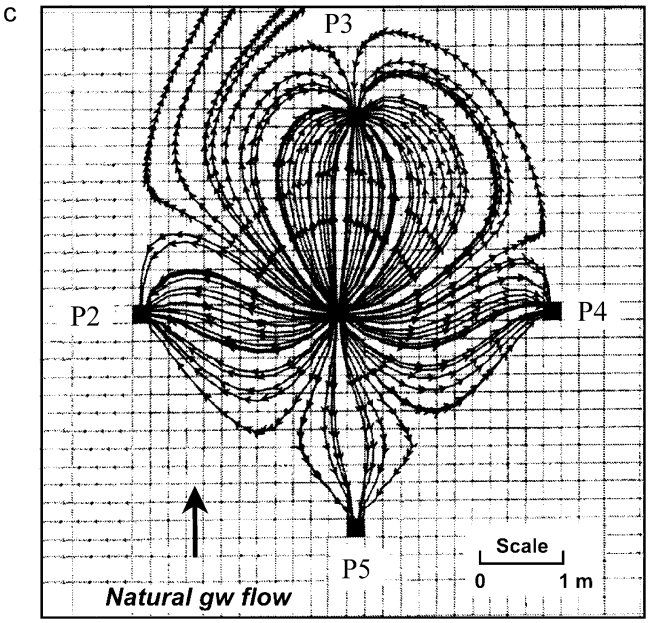

Fig. 8 (*continued*).

ratio of 1:4). The particles go slightly out of the cell in the downstream direction but are all recovered by the pumping wells. This injection-pumping rate ratio allows the sweeping of only 75% of the cell area. Two areas between the well P5 and wells P2 and P4 are not swept by the particles. In addition, with this ratio, the generated effluent is four times the injected volume. That gives a large volume of effluent to be treated. For this case, the injection rate is not sufficient to obtain good sweep efficiency. On the other hand, if the injection rate is 2.0 l/min (injection/pumping ratio of 1:1; Fig. 8b), more than 25% of the particles are not recovered by the pumping wells and the injected solution is flowing out of the experimental cell in the downstream direction. Therefore, this pumping ratio was not used for the test. In the simulation with an injection rate of 1.0 l/min (injection/pumping ratio of 1:2; Fig. 8c), all the cell is contacted by the injected fluid. The simulation shows also a small loss of about 4% of injected solution between P2 and P3. Some particles take over 1000 h to be recovered by the pumping well P3. Each arrow represents the migration of the fluid on a 20-h period. In this simulation, the number of particles is 100 instead of 400 to obtain a clearer illustration. Knowing that the field test was planned to last only 335 h, this simulation result implies that the injected fluid that will effectively be lost out of the cell is minimal. This injection-pumping rate was selected for the field test.

5. Results of the field test and discussion

5.1. Areal sweep efficiency (E_A)

The movement of the washing solution in the aquifer can be monitored using the arrival time of the solution at the observation wells determined by the visual observation of the

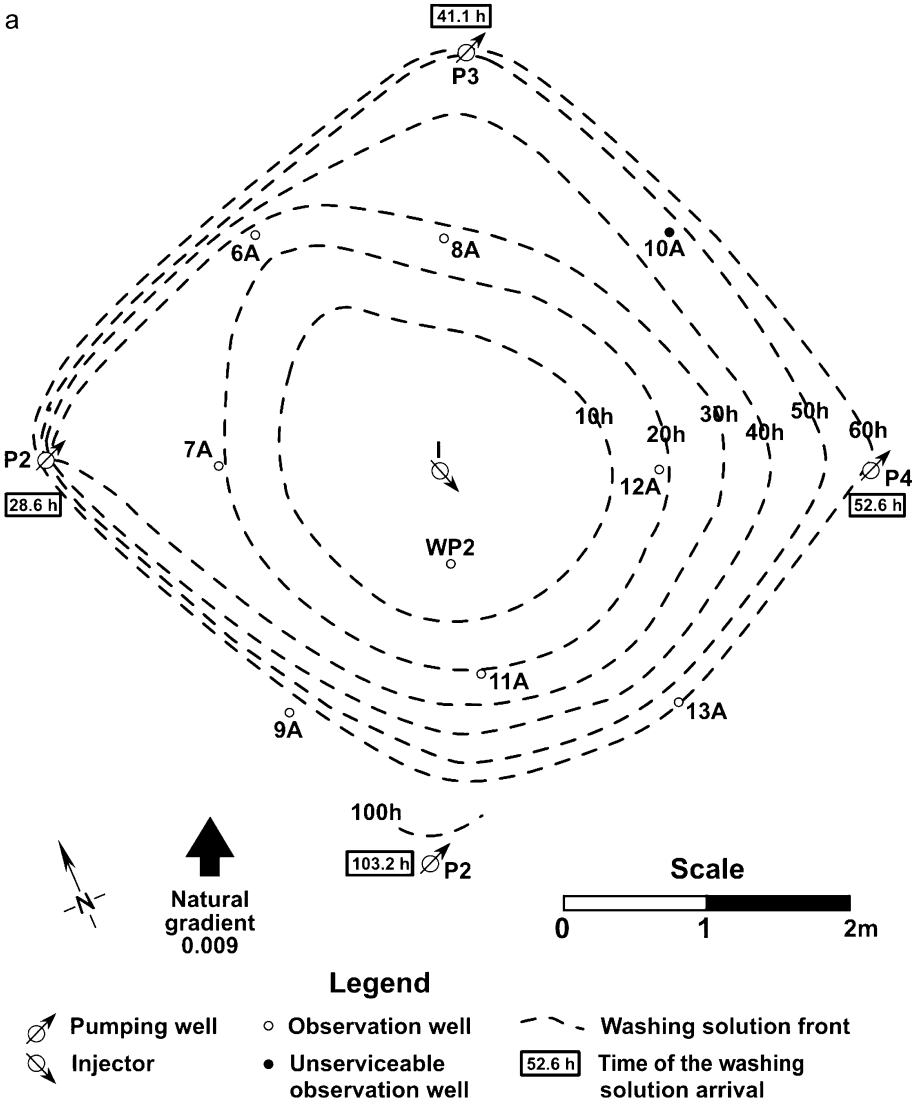

Fig. 9. (a) Areal view of the washing solution movement observed in the field. (b) Areal view of the washing solution movement calculated by numerical modeling.

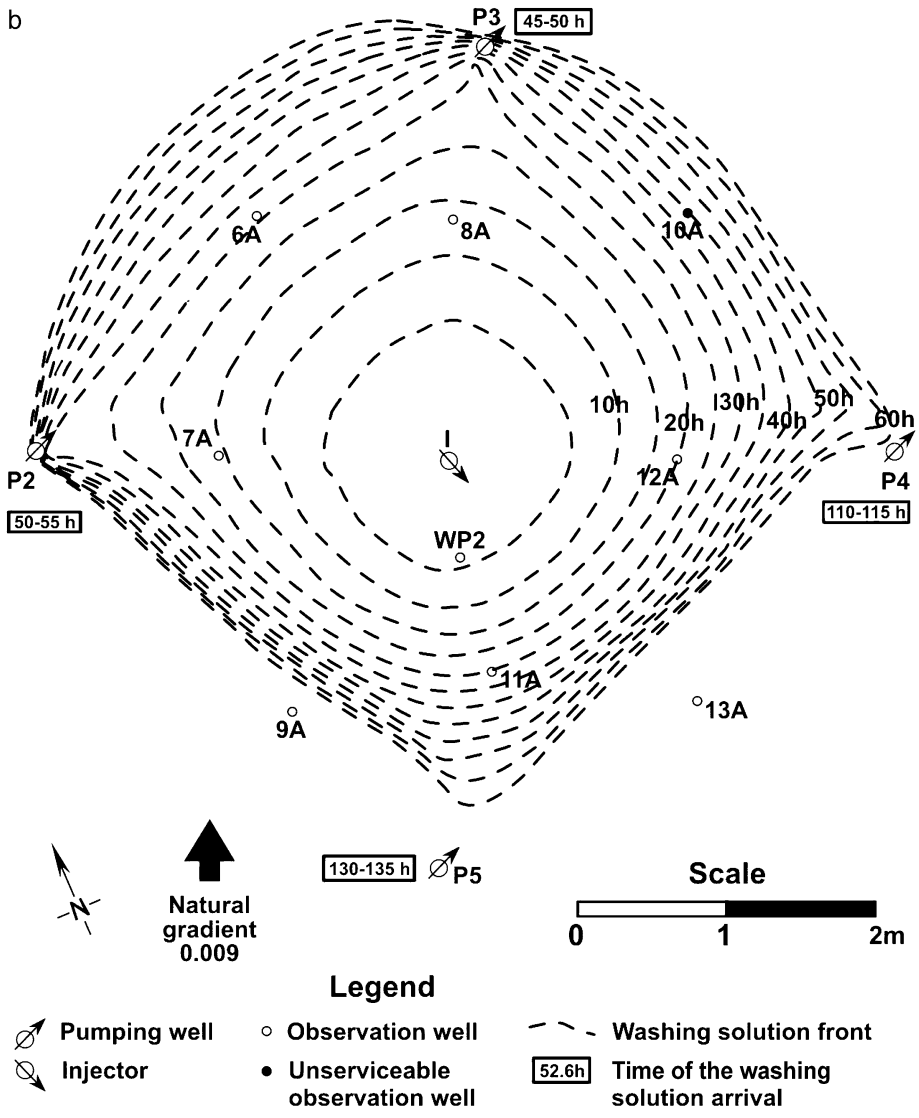

Fig. 9 (*continued*).

samples (Fig. 9a). The same movement can be simulated by numerical modeling (Fig. 9b). As predicted, the washing solution arrival at well P5 (103.2 h) is later than the one at well P3 (41.1 h) because of the effect of natural groundwater flow. The arrival times for these two wells are very close to those predicted by the simulation (Fig. 9b). On the other hand, for the wells P2 and P4, the arrival times of the washing solution are two times faster than

those simulated. This difference is probably the result of soil heterogeneity which favoured the flow to wells P2 and P4. The difference of arrival times observed between the wells P2 and P4, which are perpendicular to natural groundwater flow, can be explained by two reasons: well P2 is 0.25 m closer to the injector and the aquifer thickness becomes thinner between the injector (2 m) and the well P2 (1.6 m), whereas it becomes thicker toward well P4 (2.4 m). The cell area is completely swept by the washing solution after 100 h of injection. The areal sweep efficiency (E_A) is considered to be near 100%.

5.2. Vertical sweep efficiency (E_I)

The objective behind the use of a polymer solution in the injection sequence is to enhance the front stability between fluids in the porous medium. To verify the effect of adding xanthan gum in water on mobility control, two conservative tracers were introduced in the injected fluids. Chloride ions (Cl^-) were added to a water slug that pushes another water slug and bromide ions (Br^-) were added to the polymer solution slug that pushes the preceding water slug containing chlorides. The tracer concentrations were analysed in water samples collected in wells WP2 and 11A2. The chlorides and bromides monitored in those observation wells are drawn as a function of PV in Fig. 10a and b. Tracer breakthrough curves in water (Cl^-) and a 0.2 g/l xanthan gum solution (Br^-) show a similar behaviour at a radial distance of 0.65 m from the injector. The high shear rates close to the injector due to the high fluid velocity (see Fig. 7) reduced the viscosity of the polymer solution and made this solution to behave similar as water (Fig. 10a). There is thus no obvious polymer effect close to the injection well. At 1.4 m from the injector (Fig. 10b), the bromide breakthrough curve associated to the polymer solution shows a sharper front compared to the chloride breakthrough curve associated to the water flooding. The polymer solution had a positive effect on front stability at a certain distance from injection well. To maintain this positive effect closer to the injector well, contrary to what was observed in well WP2 (Fig. 10a), the injection rate should be maintained minimal at the beginning of the injection of the polymer solution following the washing solution

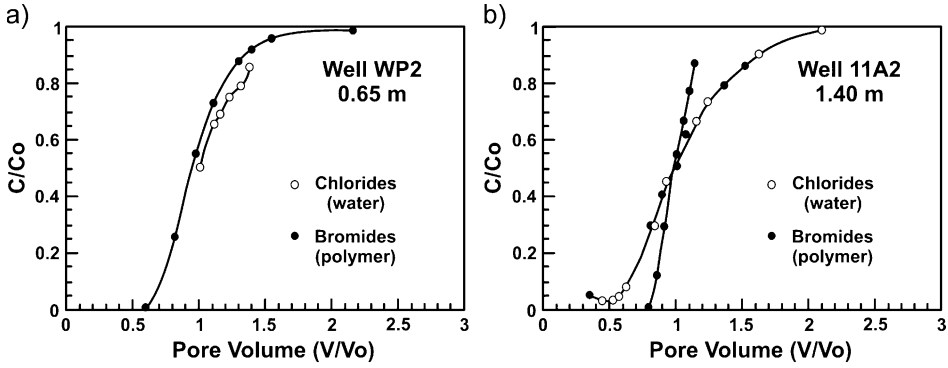

Fig. 10. Breakthrough of chlorides (water) and bromides (polymer) at 0.65 m (a) from the injector and at 1.4 m (b) from the injector.

injection. Such a slow injection rate would avoid shear thinning effects of the polymer solution, maintain a sharp displacement front ahead of the polymer solution, and thus prevent dilution of the washing solution by fingering.

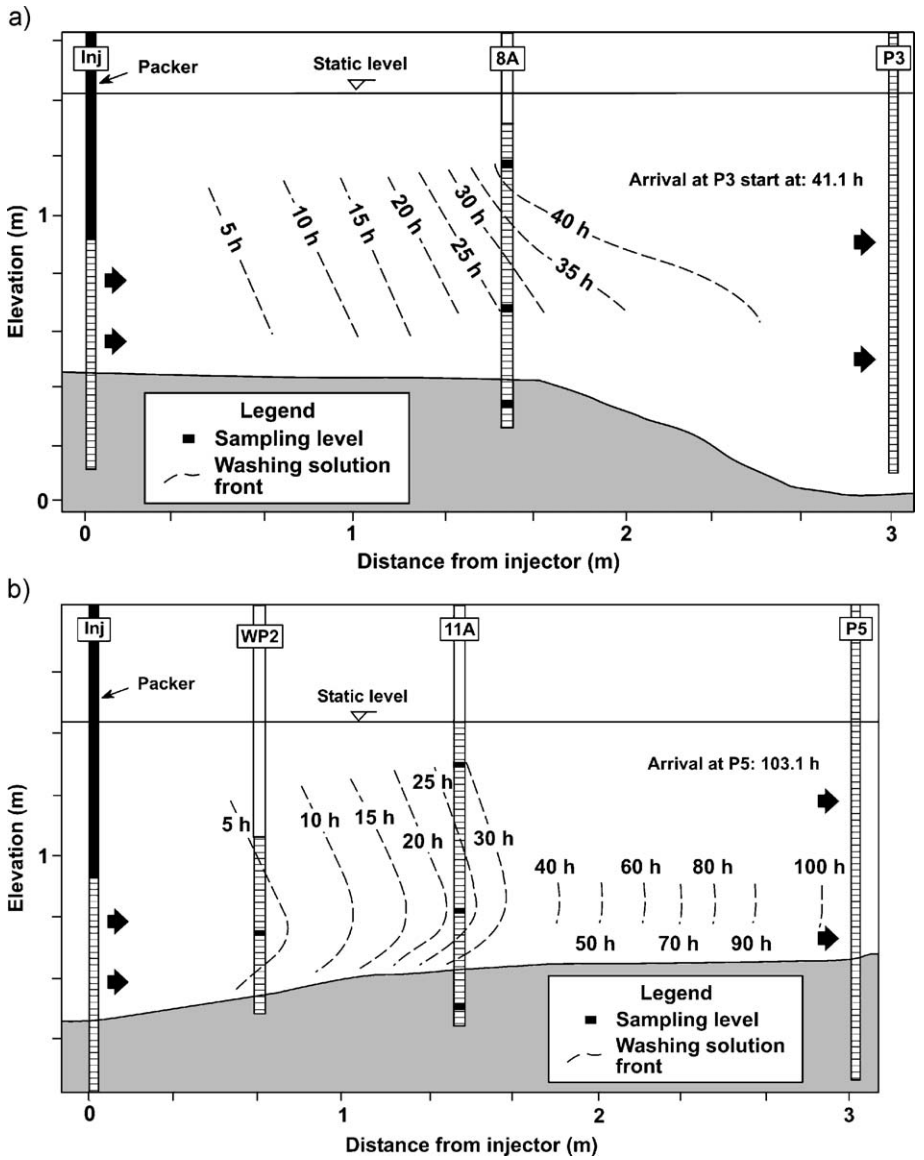

Fig. 11. (a) Washing solution movement as a function of time for the cross-section between the injector and the well P3. (b) Washing solution movement as a function of time for the cross-section between the injector and the well P5. (c) Washing solution movement as a function of time for the cross-section between the injector and the well P4.

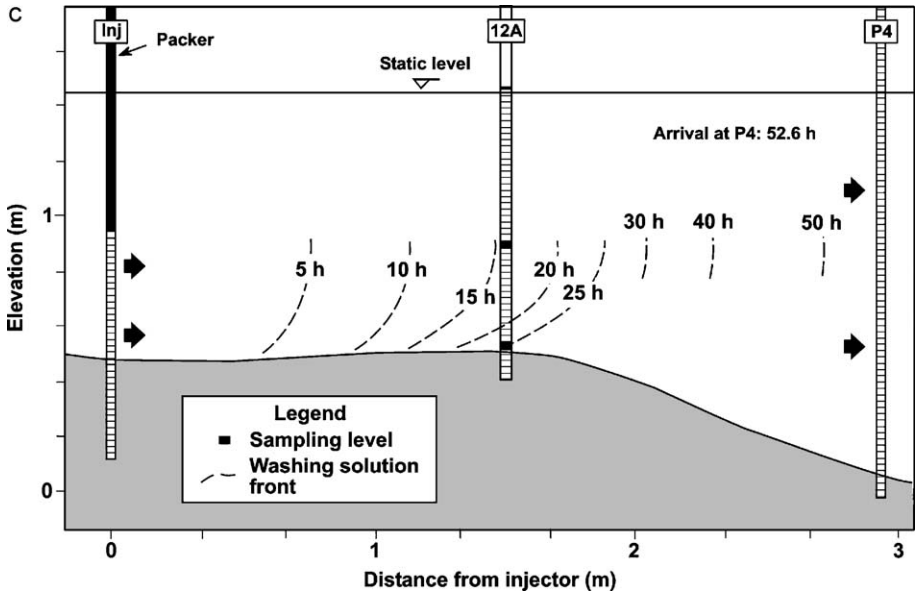

Fig. 11 (*continued*).

As for the areal sweep, the washing solution front was also observed in cross-section between the injector and the pumping wells to assess the vertical sweep efficiency (E_I). Fig. 11a, b and c shows a cross-section parallel to the groundwater flow direction. It shows the location of sampling points and the position of the washing solution front according to the observation of the fluid samples collected as a function of time. Fig. 11a shows a delay, close to P3, in the washing solution movement at the top of the aquifer. In Fig. 11b, the circulation of the fluids is in the opposite direction of the natural gradient and can explain the late arrival of the washing solution at P5. In both figures, the curved shape of the front is related to heterogeneity in sand permeability and NAPL saturation. The evaluation of permeability from grain size analysis of soil samples shows that the sand permeability is smaller below the silt layer and above the clay base of the aquifer (Hébert, 1999). Furthermore, NAPL saturation is higher below the silt layer which decreases the relative permeability to the circulating fluids (Martel et al., 1998d). In a cross-section perpendicular to the natural groundwater flow direction, the same front behaviour is observed (Fig. 11c). Cross-sections show that, after 100 h of injection, almost all of the total thickness of the cell is contacted by the washing solution. Almost the entire vertical profile of the test cell was swept by the washing solution. The nonswept zones are located at depth in the sand formation around P3 and P4 where the clay base is deeper and just below the silt layer around P3. Based on these profiles, the vertical sweep efficiency is estimated to be 95% after 100 h of injection.

5.3. Volumetric sweep efficiency

Combining the areal sweep efficiencies (E_A) and vertical sweep efficiencies (E_I) estimated after 100 h of injection and considering that the injection was done over a period of 200 h after the beginning of the washing solution injection, it is possible to conclude that the volumetric sweep efficiency (E_V) is around 95%. This estimation is well above the E_V value of 40% to 60% observed during the water flooding of petroleum reservoirs (Lake, 1989), indicating that the injection-pumping pattern selected and the use of polymer solution can play an important role in the volumetric sweep of an aquifer during soil washing.

5.4. Displacement efficiency

Based on a mass balance of the DNAPL present in soil before and after the field test, we estimated that 86% of the initial NAPL saturation was recovered (Martel et al., 1998d). This value represents the recovery efficiency (E_R) of the test. We also know, as evaluated above, that the volumetric sweep efficiency (E_V) of the test was 95%. With the displacement efficiency (E_D) being the recovery efficiency (E_R) divided by the volumetric sweep efficiency (E_V), we can estimate E_D at 90% [Eq. (1)]. This average value of the displacement efficiency for the field test is above what was anticipated from the DNAPL recovery in a sand column test. In a laboratory test done with the sand and the DNAPL from the site with the same washing solution injected downward at field temperature, only 80% of the residual DNAPL saturation was removed by dissolution after the injection of more than 4 PV of washing solution. The increase in recovery in the field test compared to the lab can be explained by the difference in initial DNAPL saturation in the sand, which was 0.27 in the field test and only 0.12 in the sand column test. A higher DNAPL saturation increases the potential for DNAPL mobilisation.

5.5. Recovery mechanisms

This section explains the recovery mechanisms observed in fluid samples collected from two observation wells located at a radial distance of 0.65 m (WP2) and 1.4 m (11A2) from the injection well. The main objective of the field experiment was to recover DNAPL by dissolution. Phase diagram optimisation done to select the washing solution was oriented on that purpose (Martel et al., 1998b). However, the addition of solvents to the washing solution that was done to enhance dissolution also lead to an important mobilisation potential due to the transfer of solvents into the DNAPL. A heterogeneous distribution of the DNAPL saturation and especially the presence of DNAPL pools may have contributed to the mobilisation of the DNAPL when they were contacted by the washing solution as observed by Conrad et al. (submitted for publication) and Robert et al. (2001).

Fig. 12 presents a picture of the liquid samples collected in the observation well WP2 (0.65 m from the injection well) during the washing solution injection. The first three samples on the left represent the washing solution breakthrough. The dilution at the front creates a macroemulsion of surfactant–alcohol–solvent in water without DNAPL. The

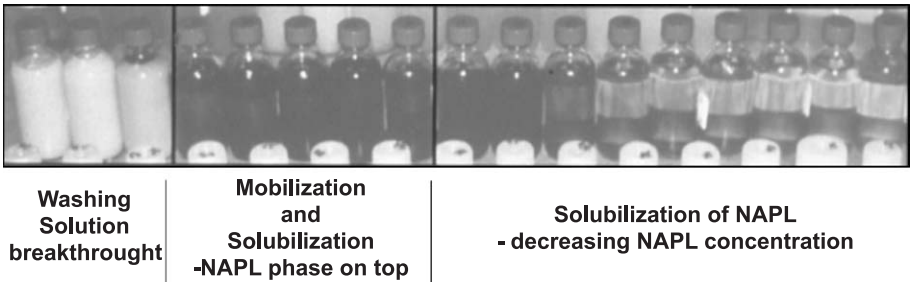

Fig. 12. Liquid samples collected in the observation well WP2 at 0.65 m from the injector during washing solution injection.

next five samples have two phases: a NAPL phase on the top (8% to 20% in volume) containing about 60% of NAPL and a NAPL-in-water microemulsion containing from 0.5% to 3.24% of NAPL. The next samples have a single phase of NAPL-in-water microemulsion with NAPL concentrations decreasing from 1.82% to 0.07%.

Fig. 13 shows the NAPL proportion recovered in the samples collected at WP2 and 11A2 as a function of the volume of washing solution circulated (V/Vo where Vo is the respective pore volume at 0.65 m or at 1.4 m from the injector) for the two observation wells. Fig. 13 shows clearly the main recovery mechanism involved in each monitoring well. At 0.65 m (WP2), the maximum NAPL recovery is by mobilisation ahead of the washing solution breakthrough, i.e., before 1 PV of injected solution (dotted line on Fig. 13). This is the NAPL bank formed by partial NAPL mobilisation ahead of the washing

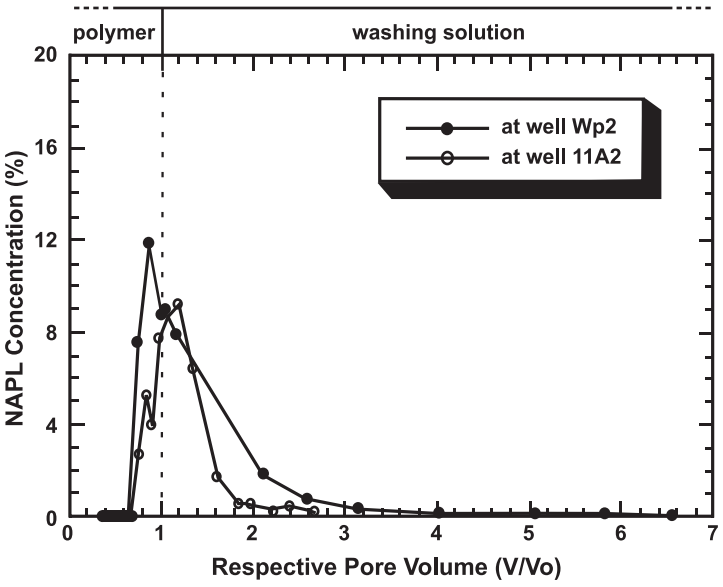

Fig. 13. NAPL concentration as a function of pore volume at 0.65 Wp2 and 1.4 11A2 m from the injection well.

solution. At 1.4 m (11A2), the maximum NAPL recovery is occurring after the washing solution breakthrough by dissolution of the NAPL in the surfactant solution bank. For the well WP2, the first five samples, containing the mobile phase, are the only ones with more than 5% of NAPL (7.6 to 11.8%). The majority of the NAPL recovery (93%) is done at the

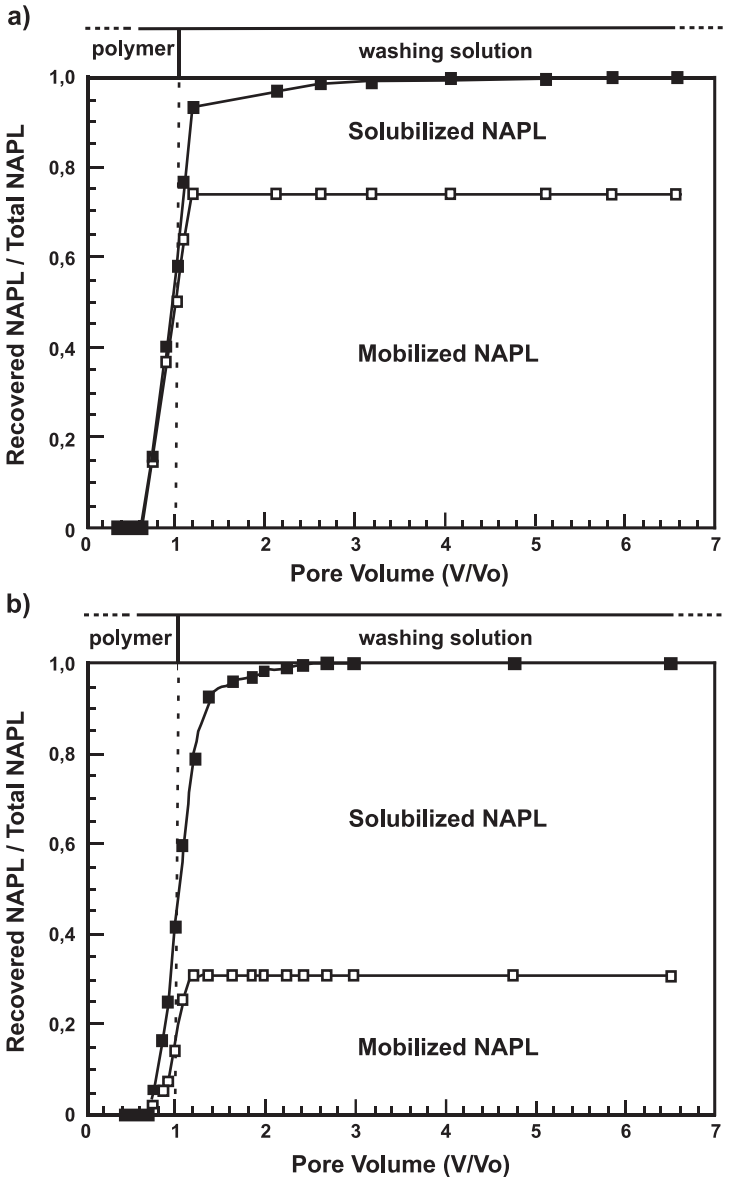

Fig. 14. Proportion of NAPL recovered by mobilisation and solubilisation (a) at 0.65 m (Wp2) from the injector and (b) at 1.4 m (11A2) from the injector.

washing solution breakthrough, with 0.44 PV (between 0.74 and 1.18 PV) present in a NAPL bank. At 1.4 m from the injector, the recovery is less efficient: 79% of NAPL is recovered with the same pore volume circulated (between 0.76 and 1.19 PV). However, for this well, the sample following the NAPL bank contains 6.4% of NAPL in water giving the same NAPL recovery (92%) as above but with more fluid circulation (0.62 PV: between 0.74 and 1.36 PV) because the recovery mechanism is mainly dissolution.

Fig. 14a shows the proportion of NAPL recovered by dissolution and mobilisation at 0.65 m from the injector. For this well, nearly 75% of the NAPL is recovered by mobilisation. At 1.4 m from the injection well, the mechanism responsible for 70% of the NAPL recovered is instead dissolution whereas 30% of NAPL is recovered by mobilisation (Fig. 14b).

In both observation wells (WP2 and 11A2), a mobilised NAPL phase has been observed between 0.75 PV and 1.2 PV. However, the proportion of NAPL phase in the samples was different: from 8% to 20% by volume at 0.65 m and from 3.1% to 6.8% by volume at 1.4 m. The contrary was observed for the dissolved concentration: the maximum proportion of dissolved NAPL in the samples is 3.24% at 1.18 PV at 0.65 m whereas the maximum is 6.93% at 1.19 PV at 1.4 m.

In addition to the radial effect that influences the dimension of the mobilised NAPL bank, it is probable that a longer contact time of the washing solution with DNAPL promoted its dissolution at well 11A2. The velocity profile calculated in the porous medium during the washing solution injection shows that the fluid velocity at 1.4 m is one-third of the one at 0.65 m (Fig. 7).

In summary, the increase in the dissolved NAPL proportion in samples at 1.4 m shows that the fluid velocity has an effect on the recovery mechanisms by changing the capillary number of the displacement (for the mobilisation) and the contact time between the washing solution and the NAPL (for the solubilisation). For a fluid velocity three times lower, the main NAPL recovery mechanism changed from 75% by mobilisation (0.65 m from the injector) to 70% by dissolution (1.4 m from the injector).

6. Conclusions

The L'Assomption field test revealed the importance of slug sizing when a radial injection geometry is used, especially for a low-volume and high-concentration micellar washing solution. The use of an injection-pumping pattern allowing a complete sweep of the cell is critical for an optimum NAPL recovery. Further on, washing solution slug sizing is necessary to obtain the optimal displacement efficiency. Following a good characterisation, numerical simulation is an efficient mean to evaluate the injection-pumping pattern and to optimise pumping and injection rates.

The five-spot pattern used in the L'Assomption field test provided a very good volumetric sweep of the cell mainly due to the use of polymer solutions. More than 95% of the cell was contacted after 100 h of injection, although the radial pattern involved a slug thinning effect and a flow velocity variation as a function of distance from the injector. A linear pattern as used by Londergan et al. (2001) would have probably provided a more uniform volumetric sweep and a better control on flow velocity. But the five-spot technique permitted a better confinement of the test.

The polymer solution was efficient to improve volumetric sweep and mobility control. A prewash polymer solution was used to homogenise the advancing washing solution because of the shear thinning effect and to fill potential adsorption sites. A second polymer solution slug with a decreasing viscosity allowed enhancing the mobility control when the washing solution was pushed. At middistance between the injector and the pumping wells, a solution with polymer has presented a better front stability than water slug in lowering the effects of dispersion.

The polymer solution has a positive effect on front stability at a certain distance from injection well. However, due to shear thinning effects, the injection rate must be minimal at the beginning of the injection of the polymer solution following the washing solution injection to maintain the beneficial effect of the polymer solution and prevent dilution of the washing solution by fingering.

The study of NAPL recovery processes showed two main recovery mechanisms: (1) mobilisation in front of the washing solution and (2) dissolution in the washing solution slug. At 0.65 m from the injector, close to 75% of the NAPL recovery was mobilised, whereas at 1.40 m, this proportion fell to 30%. Radial effect of the pattern implied also that the NAPL bank was thinning as the distance to the injector increased and the relative proportion of mobilised NAPL volume is decreased. On the other hand, the radial pattern involves a major flow velocity reduction (velocity at 1.40 m is one-third of the one at 0.65 m) as a function of distance from the injector. The reduced velocity leads to an increase in the contact time of the washing solution with the in situ DNAPL and enhanced its dissolution.

Acknowledgements

This project was funded by the DESRT program (Environment Canada and Environment Québec) and Natural Sciences and Engineering Research Council of Canada (NSERC). We would like to thank the graduate students for their assistance during the field work (Dominique Marceau, Karl-Éric Martel, Pierrette Vaillancourt, René Dufault, Nathalie Roy, Mireille Lapointe, Julie Simard and Lucie Gauthier). A special thanks to Catherine Blais who performed the chemical analysis work in the laboratory and to Yvon Couture and Linda Lecours from Environment Québec for their analytical support in the field.

Appendix A. Ogata–Banks solution in radial form

The Ogata–Banks solution was used to estimate the relative concentration profile of the injected washing solution in a radial system between a central injection well and a production well for the miscible displacement with dispersion of the fluids present in the system by the injected fluid (Fig. 5). The original equation of Ogata and Banks (1961) represents a solution of the advection–dispersion equation for a constant velocity miscible displacement in a semi-infinite, one-dimensional linear system for an initial condition of zero concentration in the system: $C(x) = 0$, $\forall\ x > 0$ at $t = 0$, if x (m) is used to represent the one-dimensional distance from the origin of the system, $x = 0$, where injection takes place and t (s) is time. The boundary condition is the injection of a constant concentration fluid

at the origin of the system after time zero: $C(0)=C_0$ for $t>0$. A simplified form of the solution when no retardation occurs can be expressed as follows (de Marsily, 1986):

$$\frac{C}{C_o}=\frac{1}{2}\mathrm{erfc}\left(\frac{x-vt}{2\sqrt{\alpha vt}}\right) \tag{A1}$$

Where erfc is the complementary error function, v is the fluid pore velocity, and α is the longitudinal dispersivity (m). This equation can be expressed in terms of the relative pore volume PV (dimensionless), which is the injected pore volume of fluids injected in the system PV_i (m^3) over the total pore volume PV_t (m^3) contained by the system. In a linear system, the distance reached by the advection front d (m) is the product of velocity and time ($d=vt$), and thus the injected pore volume is given by the product of velocity, time, cross-sectional area (A, m^2) and porosity (n, dim.; $PV_i=vtAn$). The total pore volume in the system is the product of the total length of the system, L (m), by cross-sectional area and porosity ($PV_t=LAn$). Using such definitions, Eq. (A1) can be expressed as follows after multiplying the operator of erfc by L/L:

$$\frac{C}{C_0}=\frac{1}{2}\mathrm{erfc}\left(\frac{x/L-PV}{2\sqrt{\mathrm{PV}/Pe}}\right) \tag{A2}$$

where Pe (dim.) is the Peclet number and is defined as $Pe=L/\alpha$ (de Marsily, 1986). The term x/L is the relative distance in the system (equivalent to relative pore volume) at which the relative concentration C/C_0 is calculated. In our case, we consider the end of the system; thus, if we considered a linear system we would have $x/L=L/L=1$. Instead of a linear system, we want to represent the radial injection of fluids from a central well. The transformation of a 1D linear advection dispersion (Ogata–Banks) equation to a radial one was done previously by Butler (1991). For such a radial system, the radial distance from the origin (injection well) is represented by r (m), the total radial size of the system (at production wells) is R (m), and the thickness b (m) is constant. The relative pore volume PV is again expressed as the ratio of the injected pore volume of fluids PV_i over the total pore volume PV_t contained by the system. These terms are, respectively $PV_i=\pi r^2bn$ and $PV_t=\pi R^2bn$ and thus $PV=r^2/R^2$. In a radial system, the term x/L in Eq. (A2) that was equivalent to relative pore volume thus becomes r^2/R^2 (this term is equal to unity when the solution is calculated for the end of the system where $r=R$) and the simplified Ogata–Banks solution for a radial system is expressed as follows:

$$\frac{C}{C_0}=\frac{1}{2}\mathrm{erfc}\left(\frac{r^2/R^2-PV}{2\sqrt{\mathrm{PV}/Pe}}\right) \tag{A3}$$

To represent the problem of the relative concentration profile for an injected slug of finite relative pore volume dimensions, the superposition principle is used. For example, Fig. 5a represents the conditions for the injection of a 0.25 PV slug. We show the calculation for a normalised radial distance r/R of 0.8 and conditions for a Peclet number Pe of 200. After the injection of 0.75 PV of fluids, the washing fluid with $C/C_0=1$ was injected for the first 0.25 PV followed by 0.50 PV of $C/C_0=0$ fluid. This can be represented using the superposition principle by the injection of

0.75 PV at $C/C_0 = 1$ followed by 0.5 PV at $C/C_0 = 0$ and the calculation is done as follows:

$$\frac{C}{C_0} = \frac{1}{2}\mathrm{erfc}\left(\frac{0.8^2 - 0.75}{2\sqrt{0.75/200}}\right) - \frac{1}{2}\mathrm{erfc}\left(\frac{0.8^2 - 0.50}{2\sqrt{0.50/200}}\right) = 0.87 \quad \text{(A3)}$$

References

Blanford, W.J., Barackman, M.L., Boving, T.B., Klingel, E.J., Johnson, G.R., Brusseau, M.L., 2001. Cyclodextrin-enhanced vertical flushing of a trichloroethene contaminated aquifer. Ground Water Monit. Remediat. 21, 58–66.

Brandes, D., Farley, K.J., 1993. Importance of phase behavior on the removal of residual DNAPLs from porous media by alcohol flooding. Water Environ. Res. 65, 869–878.

Butler, R.M., 1991. Thermal Recovery of Oil and Bitumen. Prentice–Hall, Englewood Cliffs, NJ xvi, 528 pp.

Carreau, P.J., 1972. Rheological equations from molecular network theories. Trans. Soc. Rheol. 16, 99–127.

Chauveteau, G., Zaitoun, A., 1981. Basic rheological behavior of Xanthan Polysaccharide solutions in porous media: effects of pore size and polymer concentration. European symposium on enhanced oil recovery. Bournemouth, England, pp. 197–214.

Conrad, S.H., Glass, H.C., Peplinski, W.J., 2001. Bench-scale visualization of DNAPL remediation processes in analog heterogeneous aquifers: surfactant floods, and in situ oxidation using permanganate. J. Contam. Hydrol. (submitted for publication).

de Marsily, G., 1986. Quantitative Hydrogeology—Groundwater Hydrology for Engineers. Academic Press, San Diego. 440 pp.

Falta, R.W., 1998. Using phase diagrams to predict the performance of cosolvent floods for NAPL remediation. Ground Water Monit. Remediat. 19 (3), 1–9.

Falta, R.W., Lee, C.M., Brame, S.E., Roeder, E., Coates, J.T., Wright, C., 1999. Field test of high molecular weight alcohol flushing for subsurface nonaqueous phase liquid remediation. Water Resour. Res. 35, 2095–2108.

Gelhar, L.W., Mantoglou, A., Welty, C., Rehfeldt, K.R., 1985. A review of field-scale physical solute transport processes in saturated and unsaturated porous media: Electric Power Research Institute EPRI EA-4190 Project 2485–5. 116 pp.

Grubb, D.G., Sitar, N., 1999. Horizontal ethanol floods in clean, uniform, and layered sand packs under confined conditions. Water Resour. Res. 35, 3291–3302.

Hébert, A., 1999. Étude du comportement des fluides lors d'un essai de décontamination in situ à l'aide d'une solution tensioactive à l'Assomption, Québec. Mémoire de maîtrise, Département de géologie et de génie géologique. Université Laval, Québec. 115 pp.

Jawitz, J.W., Annable, M.D., Rao, P.S.C., Rhue, R.D., 1998. Field implementation of a Winsor type I surfactant/alcohol mixture for in situ solubilization of a complex LNAPL as a single-phase microemulsion. Environ. Sci. Technol. 32, 523–530.

Knox, R.C., Sabatini, D.A., Harwell, J.H., Brown, R.E., West, C.C., Blaha, F., Griffin, C., 1997. Surfactant remediation field demonstration using a vertical circulation well. Ground Water 35, 948–953.

Lake, L.W., 1989. Enhanced Oil Recovery. Prentice-Hall, Englewood Cliffs, NJ. 550 pp.

Londergan, J.T., Meinardus, H.W., Mariner, P.E., Jackson, R.E., Brown, C.L., Dwarakanath, V., Pope, G.A., Ginn, J.S., Taffinder, S., 2001. DNAPL removal from a heterogeneous alluvial aquifer by surfactant-enhanced aquifer remediation. Ground Water Monit. Remediat. 21, 57–67.

Lunn, S.R.D., Kueper, B.H., 1999. Risk reduction during chemical flooding: preconditioning DNAPL density in situ prior to recovery by miscible displacement. Environ. Sci. Technol. 33, 1703–1708.

Manning, R.K., Pope, G.A. Lake, L.W., 1983. A technical survey of polymer flooding projects. US Department of Energy DOE/BETC/10327-19, Bartlesville, Oklahoma. 344 p.

Martel, K.-E., Martel, R., Lefebvre, R., Gélinas, P.J., 1998a. Laboratory study of polymer solutions used for mobility control during in situ NAPL recovery. Ground Water Monit. Remediat. 18 (3), 103–113 (Summer).

Martel, R., Gélinas, P.J., Desnoyers, J.E., 1998b. Aquifer washing by micellar solutions: 1. Optimization of alcohol/surfactant/solvent solutions. J. Contam. Hydrol. 29 (4), 319–346.

Martel, R., Lefebvre, R., Gélinas, P.J., 1998c. Aquifer washing by micellar solutions: 2. DNAPL recovery mechanisms for an optimized alcohol/surfactant/solvent solution. J. Contam. Hydrol. 30 (1–2), 1–31.

Martel, R., Gélinas, P.J., Saumure, L., 1998d. Aquifer washing by micellar solutions: 3. Preliminary field test at the Thouin sand pit (L'Assomption, Québec, Canada). J. Contam. Hydrol. 30 (1–2), 33–48.

Mercer, J.W., Cohen, R.M., 1990. A review of immiscible fluids in the subsurface:-properties, models, characterization and remediation, J. Contam. Hydrol. 6, 107-163.

McDonald, M.G., A.W. Harbaugh, 1988. A modular three-dimensional finite-difference ground-water flow model, Techniques of Water-Resources Investigations 06-A1, USGS, 576 pp.

Ogata, A., Banks, R.B., 1961. A solution of the differential equation of longitudinal dispersion in porous media. U.S. Geol. Prof. Paper 411-A.

Pennell, K.D., Pope, G.A., Abriola, L.W., 1996. Influence of viscous and buoyancy forces on the mobilization of residual tetrachlorethylene during surfactant flooding. Environ. Sci. Technol. 30, 1328–1335.

Pitts, M.J., Wyatt, K., Sale, T.C., Piontek, K.R., 1993. Utilization of chemical-enhanced oil recovery technology to remove hazardous oily waste from alluvium. SPE Int. Symp. Oilfield Chem., 33–44 (SPE/DOE paper no. 25153).

Quirion, F., Desnoyers, J., 1984. Effects of alcohols and surfactants on the lowering of the interfacial tension between water and benzene: a correlation with phase diagrams. AOSTRA J. Res. 1 (2), 97–102.

Ramsburg, C.A., Pennell, K.D., 2001. Experimental and economic assessment of two surfactant formulations for source zone remediation at a former dry cleaning facility. Ground Water Monit. Remediat. 21, 68–82.

Rao, P.S.U.C., Annable, D.M., Sillan, R.K., Dongping Dai, K.H.W.D.G., Lynn Wood, C.G.E., 1997. Field-scale evaluation of in situ cosolvent flushing for enhanced aquifer remediation. Water Resour. Res. 33, 2673–2686.

Robert, T., Conrad, S.H., Martel, R., Lefebvre, R., 2002. Visualization of TCE recovery mechanisms using micellar-polymer solutions in a two-dimensional heterogeneous sand model. Proceedings, 3nd Joint IAH–CNC and CGS Groundwater Specialty Conference, 55th Canadian Geotechnical Conf., Niagara Falls, Ontario Canada.

Robert, T., Gabriel, U., Lefebvre, R., Martel, R., 2001. TCE Recovery during in situ flushing: experimental study of the controlling parameters. In Proceedings, 54rd Canadian Geotechnical Conference, Calgary, Alta.

Roeder, E., Falta, R.W., Lee, C.M., Coates, J.T., 2001. DNAPL to LNAPL transitions during horizontal cosolvent flooding. Ground Water Monit. Remediat. 21 (1), 77–88.

Roy, N., Martel, R., Gélinas, P.J., 1995. Laboratory assessment of surfactant biodegradation in aquifers under denitrifying conditions. 5th Annual Symposium on Groundwater and Soil Remediation, Environment Canada, Toronto, Ontario, 2–5 October 1995.

Sabatini, D.A., Knox, R.C., Harwell, J.H., Wu, B., 2000. Integrated design of surfactant enhanced DNAPL remediation: efficient supersolubilization and gradient systems. J. Contam. Hydrol. 45, 99–121.

Sahoo, D., Smith, J.A., Imbrigiotta, T.E., McLellan, H.M., 1998. Surfactant-enhanced remediation of a trichloroethene(TCE)-contaminated aquifer: 2. Transport of TCE. Environ. Sci. Technol. 32, 1686–1693.

St.-Pierre, C., Martel, R., Gabriel, U., Lefebvre, R., Robert, T., Hawari, J., 2004. TCE recovery mechanisms using micellar and alcohol solutions: phase diagrams and sand column experiments. J. Contam. Hydrol, in press.

Shiau, B.-J., Sabatini, D.A., Harwell, J.H., 1994. Solubilization and microemulsification of chlorinated solvents using direct food additive (edible) surfactants. Ground Water 32, 561–569.

Simpkin, T., Sale, T., Kueper, B., Pitts, M.J., Wyatt, K., 1999. Surfactants and cosolvents for NAPL remediation. In: Lowe, D.F., Oubre, C.L., Ward, C.H. (Eds.), A Technology Practices Manual. CRC Press, Boca Raton, FL. 412 pp.

Wheat, M.R., Dawe, R.A., 1988. Transverse dispersion in slug-mode chemical EOR processing in stratified porous media. SPE Reserv. Eng. 3 (2), 466–478.

Wright, R.J., Dawe, R.A., 1983. Fluid displacement efficiency in layered porous media mobility ratio influence. Rev. Inst. Fr. Pét. 38 (4), 455–474.

Wright, R.J., Wheat, M.R., Dawe, R.A., 1987. Slug size and mobility requirements for chemically EOR within heterogeneous reservoirs. SPE Reserv. Eng. 2 (1), 92–102.

Zhen Cao, L., 1978. . Dye Stuff Chemicals, 2nd edn. Textile Industry Press, Beijing, China, pp. 309–317.